Corresponding author: Ryan J. Herringa

Other supplemental materials

Supplemental Methods

Supplementary resting state connectivity analyses were performed using a seed-based (region-of-interest or ROI) approach. For the supplementary analyses, we used ten ROIs: left and right centromedial amygdala (CMA), left and right basolateral (BLA), left and right anterior hippocampus (AntHip), left and right posterior hippocampus (PostHip), as well as left and right anterior insula (AntIns). The amygdala and hippocampus seeds were generated using the Anatomy Toolbox[1] and following methods in prior resting state connectivity studies of PTSD[2,3]. Anterior insula seeds were kindly provided by R. Sripada to match the prior resting state connectivity study in a PTSD sample[4]. Following Chen and Etkin's methods, voxels from the hippocampus seeds overlapping with the amygdala seeds were excluded from the masks[3]. All seeds were resampled to the resolution of the resting-state EPIs (3dresample) and average time series were computed for each seed (3dmaskave). Connectivity maps were generated for each subject and each seed using a linear regression (3dDeconvolve). In order to further differentiate amygdala connectivity coming from the CMA and BLA, both time series were included together within the same 3dDeconvolve command[2]. This created connectivity maps for each seed while effectively separating the contribution of each seed from each other.

At the group level and for each seed independently, a multivariate regression analysis was conducted (3dttest++) to generate group-level connectivity maps for the above-mentioned seeds including CAPS, CES, and CTQ scores. Correlation coefficients were converted to Z-scores using Fisher's-Z transformation. Multiple comparison correction was performed using Monte Carlo simulation (3dClustSim), which incorporates the estimated smoothness of the data to establish the likelihood of false positives of different cluster sizes (i.e. cluster size thresholding). The cluster threshold was 357 voxels (2 x 2 x 2mm^3) at an individual voxel threshold of $p \leq 0.005$, resulting in a corrected $\alpha \leq 0.05$.

Additionally, the analyses were repeated with the addition of depression scores (BDI) and traumatic brain injury (TBI) as covariates at the group level.

Supplemental Results

Resting state connectivity

Figure S2 shows the connectivity maps for left amygdala, left CMA and left BLA as well as the left hippocampus, left anterior and posterior hippocampus (threshold: $p = 0.005$). Connectivity maps for the contralateral seeds were similar. As seen in Figure S2, all the amygdala connectivity maps (including CMA and BLA) were similar. Namely, they showed positive functional connectivity to the contralateral region as well as the insula, ventral striatum, hippocampus, parahippocampal gyrus, and medial frontal gyrus, and negative connectivity to posterior cingulate and occipital cortex. All hippocampus connectivity maps were also quite similar (Figure S3) and showed positive connectivity with each other as well as other regions including the lentiform nucleus, insula, and thalamus.

Correlation with childhood maltreatment (CTQ total score)

CMA and BLA connectivity: Similar to the whole amygdala results CTQ negatively predicted connectivity to the insula, regions of the mPFC including vmPFC/rostral (r)ACC and dorsomedial (dm)PFC (BA 9, 10, 24, 25, 32, 38) as well as dorsolateral (dl) PFC (BA 9, 10; Figure S4a-b and Table S2). Finally, CTQ positively predicted CMA connectivity to the PCC (BA 23; Table S2).

Anterior and posterior hippocampus connectivity: CTQ negatively predicted connectivity from the anterior hippocampus to the insula (BA 13), regions of the mPFC including vmPFC/dmPFC and the rACC (BA 10, 32, 45), and dlPFC (BA 44) (Figure S4c-d, Table S2). Additionally, CTQ positively predicted connectivity from anterior hippocampus to PCC (BA 31). CTQ negatively predicted connectivity of the

posterior hippocampus to regions of the PFC such as lPFC/vmPFC/dmPFC (BA 8, 10, 11, 46) and the anterior cingulate cortex (BA 32). Finally, CTQ positively predicted posterior hippocampus connectivity to the PCC (BA 30) (Figure S4c-d, Table S2).

Anterior Insula connectivity: CTQ negatively predicted anterior insula connectivity to the thalamus and the mammilary body (Figure S7, Table S2).

Correlation with combat exposure (CES)

CMA and BLA connectivity: No significant associations with CES were observed with CMA and BLA connectivity.

Anterior and posterior hippocampus connectivity: CES negatively predicted connectivity between the anterior hippocampus and mPFC (BA 10,32; Table S2). Finally, CES negatively predicted posterior hippocampus connectivity to the dmPFC (BA 9). CES also negatively predicted anterior hippocampus connectivity to dmPFC albeit at a slightly lower voxel-wise threshold (Figure S5).

Correlation with PTSS (CAPS past month)

CMA and BLA connectivity: Similar clusters were found with the CMA and BLA seeds as with the primary amygdala seeds. CAPS scores positively predicted CMA and BLA connectivity to dACC (BA 32), regions of the mPFC including dmPFC/dlPFC (BA 9, 10, 24), IFG (BA 6, 44), and insula (Figure S6a-c, Table S2). In addition, CAPS scores positively predicted connectivity between CMA and precuneus (BA 31).

Hippocampus connectivity: CAPS scores positively predicted anterior hippocampus connectivity to the insula (BA 13), as well as regions of the PFC including dmPFC/dlPFC/vmPFC (BA 8, 9, 10, 11, 32). CAPS scores positively predicted posterior hippocampus connectivity to the dmPFC (BA 9, 10) (Figure S6d,

Table S2). Finally, CAPS scores negatively predicted posterior hippocampus connectivity to the lentiform nucleus and medial global pallidus.

References

1. Eickhoff SB, Stephan KE, Mohlberg H, Grefkes C, Fink GR, Amunts K, et al. A new SPM toolbox for combining probabilistic cytoarchitectonic maps and functional imaging data. Neuroimage. 2005 May 1;25(4):1325–35.

2. Brown VM, Labar KS, Haswell CC, Gold AL, Mid-Atlantic MIRECC Workgroup, Beall SK, et al. Altered resting-state functional connectivity of basolateral and centromedial amygdala complexes in posttraumatic stress disorder. Neuropsychopharmacology. 2014 Jan;39(2):361–9.

3. Chen AC, Etkin A. Hippocampal network connectivity and activation differentiates post-traumatic stress disorder from generalized anxiety disorder. Neuropsychopharmacology. 2013 Sep;38(10):1889–98.

4. Sripada RK, King AP, Welsh RC, Garfinkel SN, Wang X, Sripada CS, et al. Neural dysregulation in posttraumatic stress disorder: evidence for disrupted equilibrium between salience and default mode brain networks. Psychosom Med. 2012 Nov;74(9):904–11.

Table S1. Demographic and clinical variables. Note that of the 27 subjects, 17 met full criteria for combat-related PTSD.

	Average	SD	Range	Spearman's Rank Correlation (ρ)
Age	26.4	2.5	22.2-31.8	CTQ (0.39)
CAPS Past Month	40.6	21.2	2-82	BDI (0.59), CES (0.46), CTQ (0.42)
Combat Exposure Scale	17.5	9.9	0-35	CAPS (0.46)
Childhood Trauma Questionnaire	35.1	11.1	25-63	CAPS (0.42), Age (0.39)
Beck Depression Inventory	6.6	5.2	0-23	CAPS (0.59)
NART (IQ)	106.3	8.2	91-120	--

Table S2. Regression analysis results with behavioral measures using additional seed-based connectivity of amygdala and hippocampus subdivisions, and anterior insula. Positive or negative correlations with each clinical variable and seed connectivity are indicated by + or – and were significant at $p \leq 0.05$ corrected. "Original raw connectivity" describes the sign of the raw connectivity between the ROI seed and the cluster of interest. *, significant original raw connectivity between the regions ($p \leq 0.05$ corrected). CMA = centromedial amygdala, BLA = basolateral amygdala, Ant = anterior, Post = posterior, Ins = Insula, mPFC = medial prefrontal cortex, Hip = hippocampus, PCC = posterior cingulate cortex, dlPFC = dorsolateral prefrontal cortex, dmPFC = dorsomedial prefrontal cortex, lPFC = lateral prefrontal cortex, vmPFC = ventromedial prefrontal cortex, dACC = dorsal anterior cingulate cortex, MTG = Middle Temporal Gyrus, IFG = inferior frontal gyrus, SMA = supplementary motor area.

Behavior Scale	Seed	Cluster Location	Brodmann Areas	Original Raw Connectivity	x	y	z	Peak Z	Cluster voxels
CTQ									
+	L. Post. Hip.	Right PCC	30	Positive*	-30	44	2	5.4	1089
	L. Ant. Hip.	PCC	31	Negative*	-18	42	26	5.1	416
	R. CMA	Right PCC	23	Negative	-12	34	22	5.3	765
-	L. CMA	Right Insula, cingulate gyrus, vmPFC	38, 25, 32, 24	Positive	-52	-32	-2	-6.0	4432
	L. CMA	Left Insula	22, 44, 13	Positive	52	-12	6	-4.9	853
	L. CMA	Right MTG	20	Positive (close to zero)	-54	28	-12	-5.1	373
	R. CMA	Right Insula, Bilateral cingulate gyrus, Bilateral vmPFC	9, 10, 24, 32	Positive / Negative	8	-42	8	-5.9	5720
	L. BLA	Right dlPFC	9, 10	Negative	-36	-40	24	-5.8	1710
	R. BLA	Right rACC, dmPFC	8, 9, 10, 32	Negative	-16	-36	14	-5.8	1801
	L. Ant. Hip.	dlPFC, vmPFC, dmPFC, dACC, caudate	45, 44, 13, 10, 32	Negative	-48	-16	16	-6.8	8173
	L. Ant. Hip.	Insula	13	Positive	40	-4	14	-5.8	634
	R. Ant. Hip.	dmPFC	6, 9	Positive	-4	-52	34	-6.1	1769
	L. Post. Hip.	Right lPFC, dmPFC, vmPFC, ACC	46, 8, 10, 11, 32	Negative	-52	-20	10	-5.6	4492
	R. Post. Hip.	Left ACC	32	Negative (close to zero)	8	-30	0	-4.6	478
	L. Ant. Ins.	Thalamus, mammilary body		Positive	-20	28	2	-4.9	770
CES									

-	R. Ant. Hip.	Left mPFC	32, 10	Positive (close to zero)	12	-38	4	-4.6	482
	L. Ant. Hip.	Left mPFC	32, 10	Negative (close to zero)	12	-54	0	-5.6	516
	L. Post. Hip.	Bilateral dmPFC	9	Negative*	-4	-50	32	-5.1	1750
CAPS									
+	L. CMA	Bilateral dmPFC, Right dlPFC, Left dACC, Left SMA	9, 24, 32, 6	Negative	-24	-40	28	5.8	3625
	L. CMA	Left Insula, IFG	13, 44	Positive*	42	-4	16	5.1	510
	L. CMA	Left Precuneus	31	Negative*	24	34	2	4.7	394
	R. CMA	Bilateral dmPFC, Right dlPFC, Bilateral dACC	9, 32,24	Negative (close to zero)	6	-34	34	6.7	2301
	L. BLA	Left IFG, insula	6	Positive (close to zero)	48	2	20	5.9	784
	L. BLA	Left dACC	32	Negative (close to zero)	10	-10	34	5.4	767
	L. BLA	Right dlPFC	9, 10	Negative	-36	-40	24	6.1	523
	R. BLA	Bilateral dmPFC, dlPFC	9	Negative (close to zero)	20	-48	28	5.0	1207
	L. Ant. Hip.	Bilateral Insula, ACC, dmPFC, dlPFC, vmPFC	13, 9, 44, 8, 32, 11, 10	Positive (close to zero)	40	-6	14	6.1	6945
	R. Ant. Hip.	Bilateral dmPFC, Left vmPFC	9, 10	Negative	-4	-52	32	5.8	2595
	L. Post. Hip	Bilateral dmPFC	9, 10	Negative*	-4	-50	32	5.1	1262
-	L. Post. Hip.	Left Lentiform Nucleus, Lateral Global Pallidus		Positive*	22	8	-2	-4.3	506
	L. Post. Hip.	Right Lentiform Nucleus, Medial Global Pallidus		Positive*	-18	6	0	-6.1	390

Figure S1. Scatterplots show the relationship between the behavioral variables and the extracted, raw connectivity values for the functional regions of interest displayed in Figures 2-4.

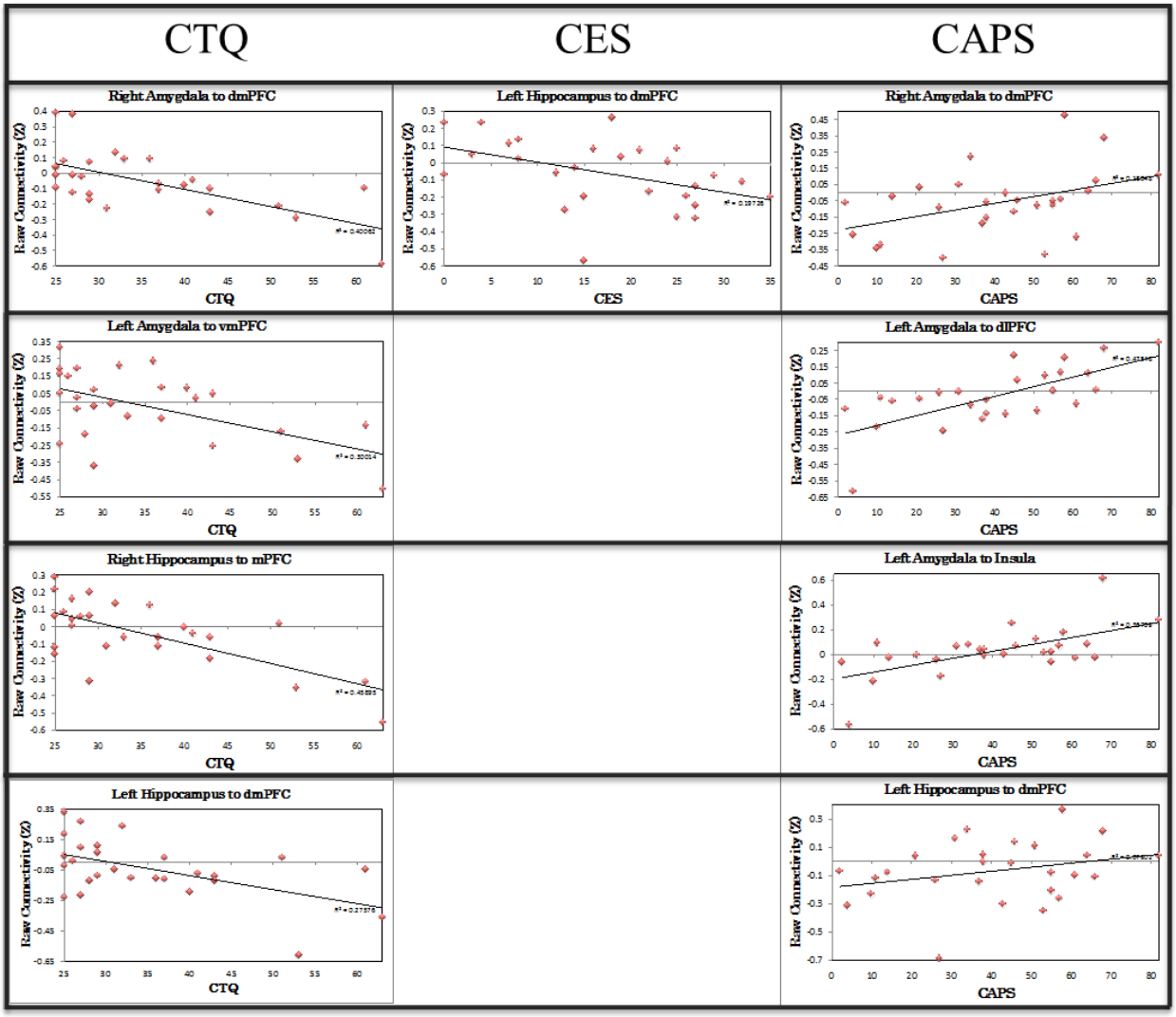

Figure S2. Functional connectivity maps showing regions that are significantly connected to left amygdala (top), left centromedial amygdala (CMA, middle), and left basolateral amygdala (BLA, bottom). Seed regions are shown on the left, with connectivity maps on the right. Connectivity maps for the right amygdala, right CMA and right BLA showed similar patterns. Positive connectivity is indicated by orange-yellow overlays, and negative connectivity by blue overlays. For axial and coronal views, the right side of the brain faces left. The connectivity map at the top is the same as the amygdala connectivity from Figure 1. Maps are displayed at voxelwise $p \leq 0.005$.

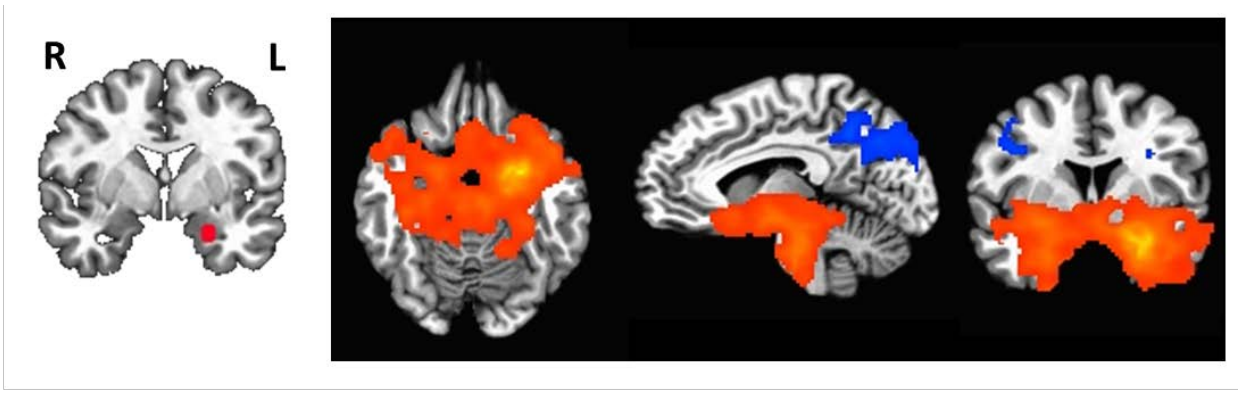
R
L

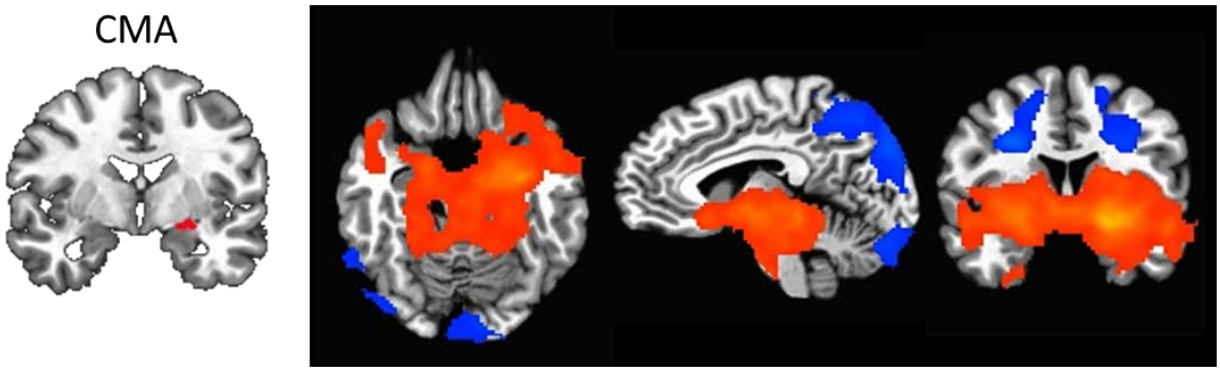
CMA

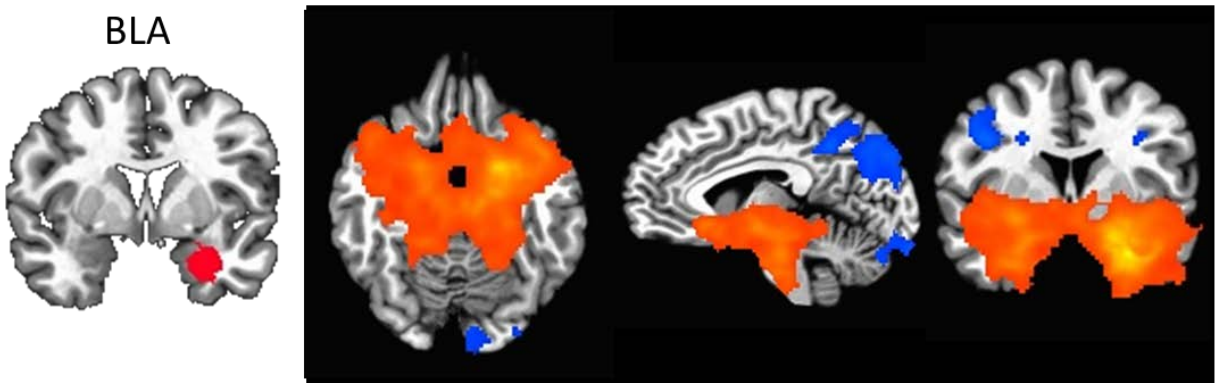
BLA

Figure S3. Functional connectivity maps showing regions that are significantly connected to left hippocampus (top), left anterior hippocampus (middle), and left posterior hippocampus (bottom). Seed regions are shown on the left, with connectivity maps on the right. Connectivity maps for the right hippocampus, right anterior hippocampus and right posterior hippocampus showed similar patterns. Positive connectivity is indicated by orange-yellow overlays, and negative connectivity by blue overlays. For axial and coronal views, the right side of the brain faces left. The connectivity map at the top is the same as the hippocampus connectivity from Figure 1. Maps are displayed at voxelwise $p \leq 0.005$.

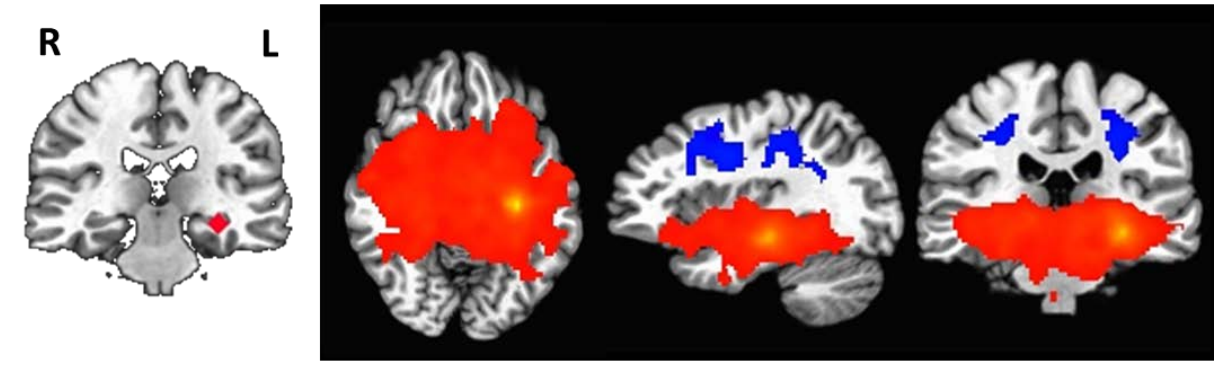
R
L

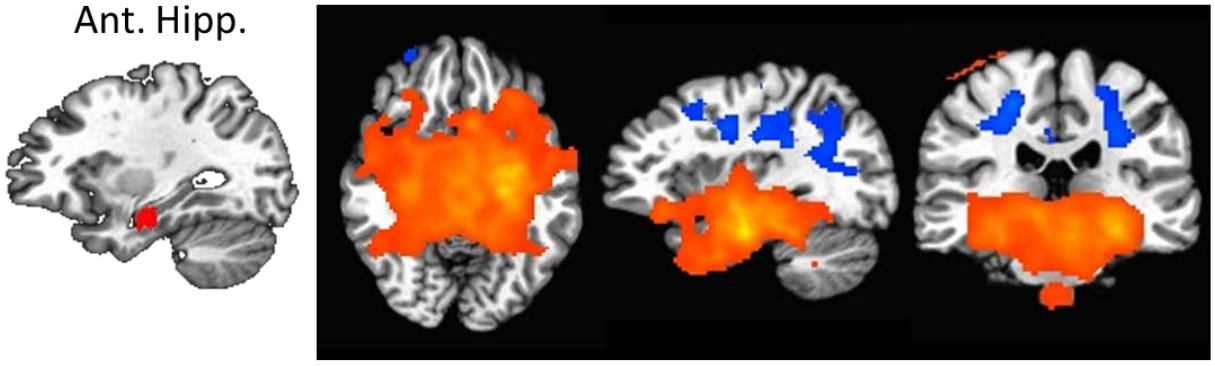
Ant. Hipp.

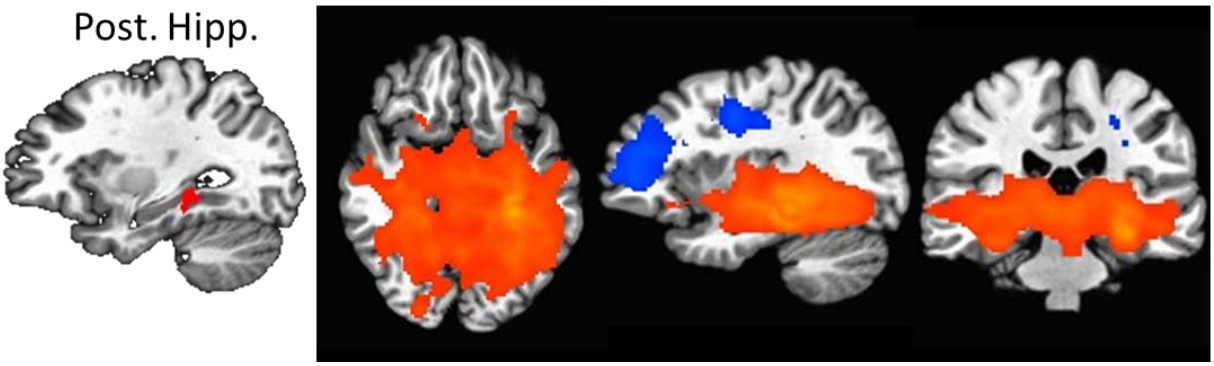
Post. Hipp.

Figure S4. Correlation between childhood maltreatment (CTQ) and resting functional connectivity of the (a,b) amygdala, centromedial amygdala (CMA), and basolateral amygdala (BLA); and (c,d) the hippocampus, anterior hippocampus, and posterior hippocampus. The images indicate the brain areas where the connectivity to the seed region is significantly correlated with CTQ ($p<0.05$, corrected). Positive correlations are indicated by orange-yellow overlays, and negative correlations with blue overlays. For axial and coronal views, the right side of the brain faces left. The maps at the top are the same as the amygdala results from Figure 2. CTQ=Childhood Trauma Questionnaire, total score.

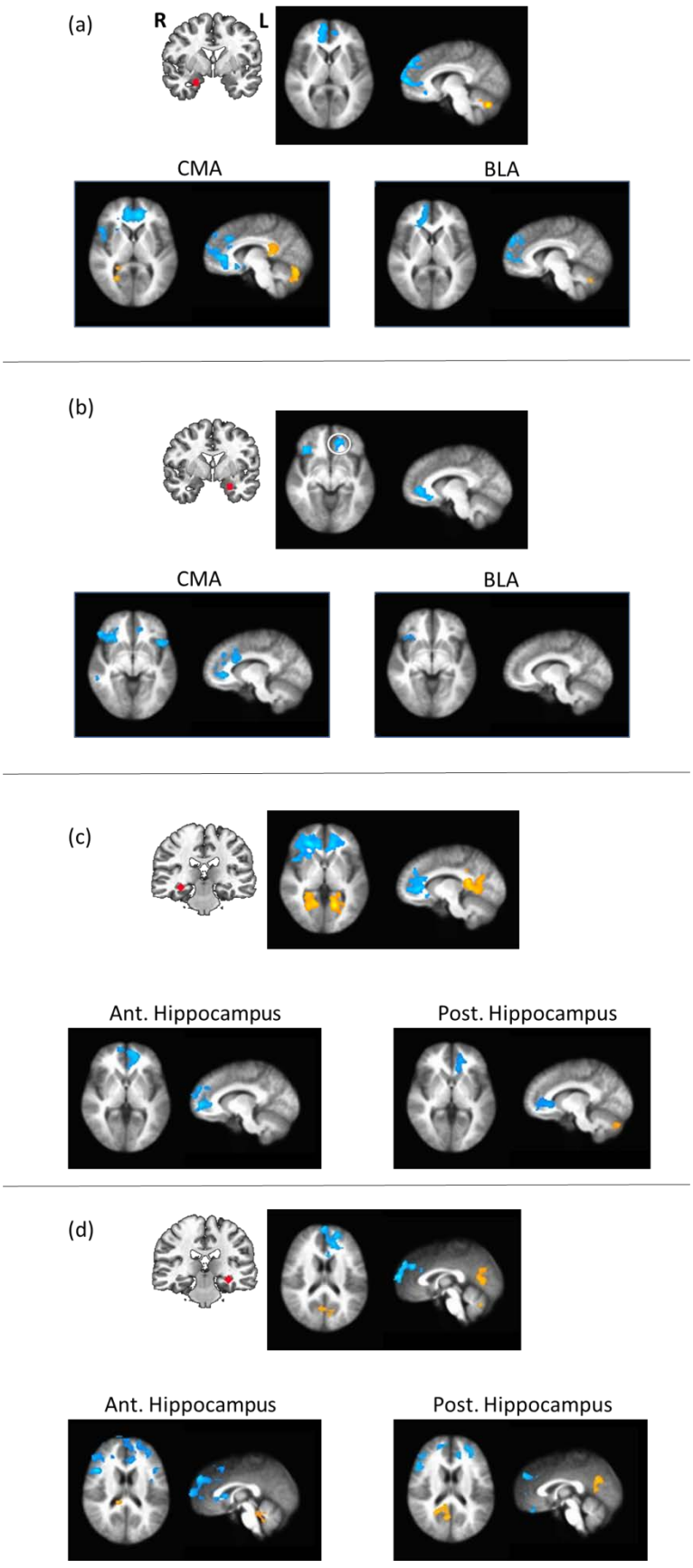
(a)
R
L
CMA
BLA
(b)
CMA
BLA
(c)
Ant. Hippocampus
Post. Hippocampus
(d)
Ant. Hippocampus
Post. Hippocampus

Figure S5. Correlation between combat exposure (CES) and resting functional connectivity of the hippocampus, anterior hippocampus, and posterior hippocampus. The images indicate the brain areas where the connectivity to the seed region is significantly correlated with CES ($p<0.05$, corrected). Positive correlations are indicated by orange-yellow overlays, and negative correlations with blue overlays. For axial and coronal views, the right side of the brain faces left. The maps at the top are the same as the hippocampus results from Figure 3. Anterior hippocampus connectivity is additionally displayed at voxel-wise $p=0.01$ to demonstrate the association with CES present at a slightly lower threshold. CES=Combat Exposure Scale.

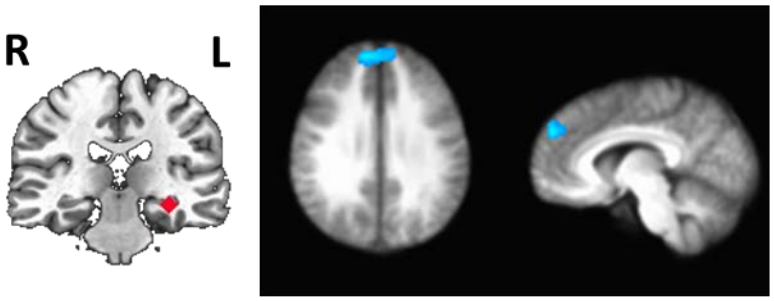

Ant. Hippocampus

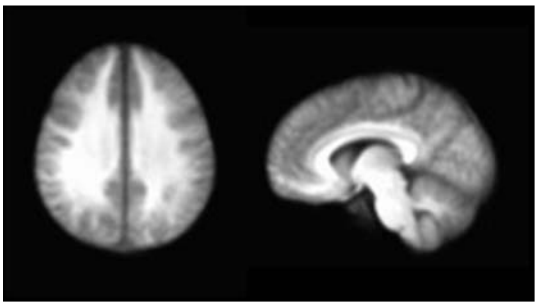

Post. Hippocampus

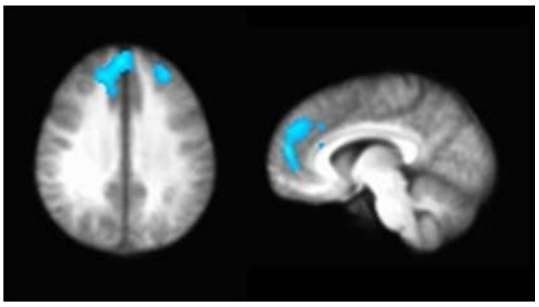

Ant. Hippocampus
(Voxel-wise p =0.01)

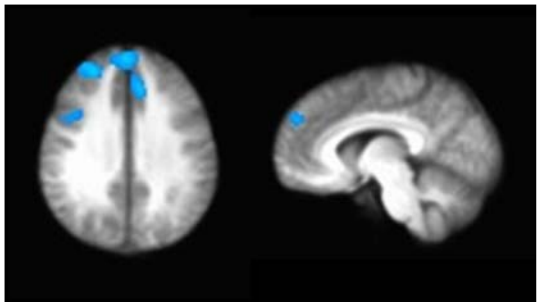

Figure S6. Correlation between post-traumatic stress symptoms (PTSS) and resting functional connectivity of the (a-c) amygdala, centromedial amygdala (CMA), and the basolateral amygdala (BLA); and (d) hippocampus, anterior hippocampus, and posterior hippocampus. The images indicate the brain areas where the connectivity to the seed region is significantly correlated with PTSS ($p<0.05$, corrected). Positive correlations are indicated by orange-yellow overlays, and negative correlations with blue overlays. The maps at the top are the same as the amygdala and hippocampus from Figure 4. For axial and coronal views, the right side of the brain faces left. PTSS were based on the past month total score of the Clinician-Administered PTSD Scale (CAPS).

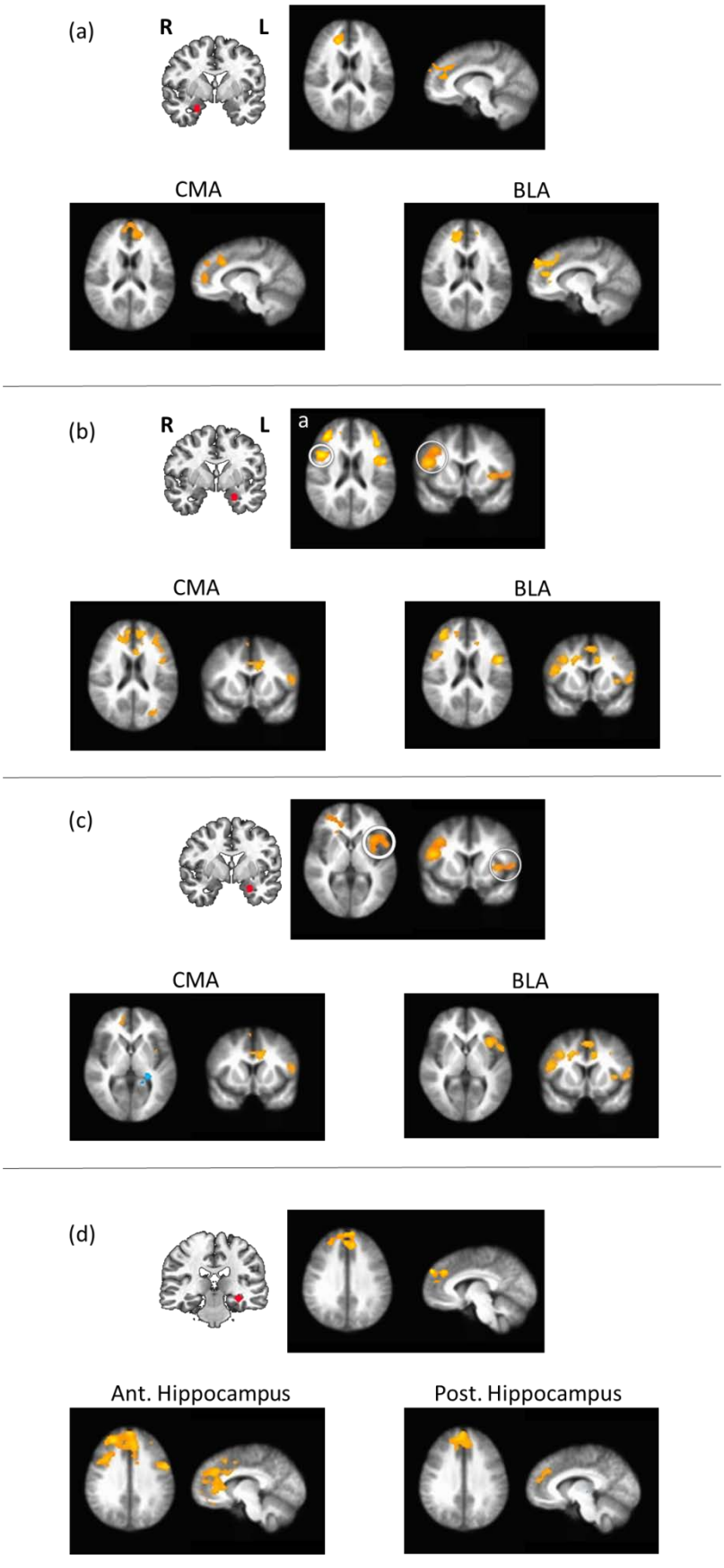
(a)
R
L
CMA
BLA
(b)
R
L
a
CMA
BLA
(c)
CMA
BLA
(d)
Ant. Hippocampus
Post. Hippocampus

Figure S7. Functional connectivity maps showing regions that are significantly connected to left anterior insula (top) and correlation with childhood maltreatment (CTQ, bottom). Seed region is shown on the left, with connectivity map on the right. General connectivity maps for the right anterior insula showed similar patterns. Positive connectivity in the top panel is indicated by orange-yellow overlays, and negative connectivity by blue overlays. In the bottom panel, the images indicate the brain areas where the connectivity to the seed region is significantly correlated with CTQ ($p<0.05$, corrected). Positive correlations are indicated by orange-yellow overlays, and negative correlations with blue overlays. For axial and coronal views, the right side of the brain faces left. Maps are displayed at voxelwise $p \leq 0.005$. CTQ=Childhood Trauma Questionnaire, total score.